Journal of the Korean Physical Society, Vol. 47, No. 1, July 2005, pp. 74∼78

Characteristics of a Pin-to-Plate Dielectric Barrier Discharge in Helium

Yong-Hyuk Lee*
Department of Materials Sciences & Engineering and Center for Nanotubes and Nanostructured Composites, Sungkyunkwan University, Suwon 440-746

Geun-Young Yeom†
Department of Materials Sciences & Engineering, Sungkyunkwan University, Suwon 440-746

(Received 6 January 2005, in final form 22 March 2005)

In this study, the characteristics of a modified dielectric barrier discharge (DBD) (that is, a pin-to-plate DBD) in He have been studied as a function of the applied AC voltage, the air gap between the electrodes, and the pin density of the powered electrode. The pin-to-plate DBD showed typical current-voltage characteristics similar to those of a corona discharge. The optimum air gap between the electrodes at a given applied voltage was 4 mm, for which the consumed power was a maximum. When the air gap was larger than 4 mm, the discharge changed from a glow discharge to a filamentary discharge. An increase in the pin density from 4 to 16 pins/cm^2 also increased the consumed power at a given voltage and at a fixed air gap. When the optical emission intensities from He metastable and oxygen atoms from the feed He gas and from the residual air, respectively were investigated by using an optical emission spectrometer, the highest optical emission intensities from He metastable and oxygen atoms was obtained for a pin density of 16 pins/cm^2 at a given voltage and a fixed air gap. The photoresist ashing rate using the residual oxygen in He was also the highest when the pin density was 16 pins/cm^2 and when the air gap was 4 mm, possibly because the dissociated oxygen atomic density in the plasma and the power consumption were highest.

PACS numbers: 50, 52
Keywords: Corona discharge, DBD, Atmospheric pressure plasma, Pin to plate, OES

I. INTRODUCTION

Atmospheric-pressure plasmas are currently applied to various processes, such as air purification, surface modification, for hydrophilic or hydrophobic properties, germ killing, *etc.* [1–4]. Also, for semiconductor and flat panel display processing, atmospheric-pressure plasmas have been studied as a replacement for wet cleaning to resolve environmental pollution due to the large quantity of liquid waste produced during wet cleaning, to cut down on operating costs such as chemical costs, to shorten the process, *etc.* [5–7]. For these purposes, among the various kinds of atmospheric-pressure plasma equipment, the plasma equipment that can generate uniform glow discharges, such as dielectric barrier discharges (DBD), capillary electrode discharges (CED), microwave discharges, plasma jets, and hollow cathode discharges, have been more widely investigated [8–12].

These days, atmospheric pressure plasmas are being investigated for applications to main flat panel display processing, such as photoresist ashing and etching, to deposition of organic and inorganic materials for diffusion barriers, *etc.*, and to the wet cleaning processing. [6, 7, 13, 14]. Currently, the etching and the deposition of flat panel display processing are mostly performed using low-pressure plasmas; however, the increasing substrate area and the advent of flexible displays for next generation flat panel displays require processing equipments having low cost of ownership, easier scalability, no vacuum processing, *etc.*, such as atmospheric pressure plasma equipment. However, if an atmospheric-pressure plasma is to be applied in the areas of etching and deposition, not only is a uniform plasma over the large area required but also a high-density plasma. In this study, as a possible application to next generation flat panel processing, a modified dielectric barrier discharge (DBD) source (named "pin-to-plate DBD") was used to generate high-density atmospheric-pressure plasmas, and the effects of multi-pin density and the gap between the electrodes on the plasma characteristics of He plasmas were investigated

II. EXPERIMENT

Fig. 1 shows the pin-to-plate DBD in-line system investigated to study the effects of multi-pin density and

*E-mail: yhlee73@skku.edu;
†E-mail: gyyeom@skku.ac.kr

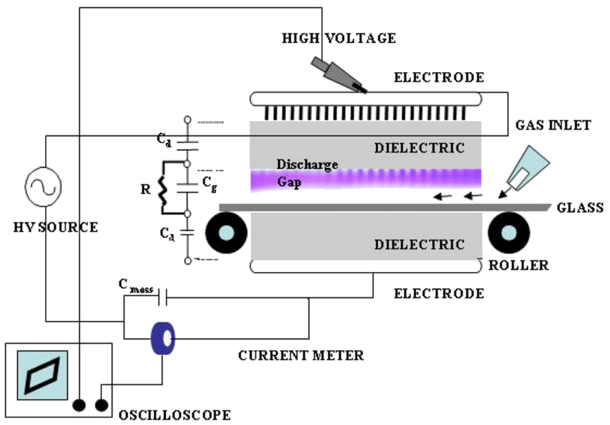

Fig. 1. The pin-to-plate DBD in-line system investigated to study the effects of the multi-pin density and the gap between the electrodes on the characteristics of atmospheric-pressure plasmas.

the gap between the electrodes on the characteristics of atmospheric-pressure plasmas. As the figure shows, the plasma source was composed of a multi-pin power electrode, a blank plate ground electrode, and a dielectric on each electrode. The thicknesses of the dielectrics was 3 mm. The size of multi-pin electrode was 100 mm × 100 mm, the multi-pin density of the electrode was varied from 4 to 16 pins/cm^2, and the gap between the dielectrics (that is the air gap) was varied from 1 to 10 mm. The atmospheric-pressure plasma source was installed in an in-line glass transport roller system; therefore, glass substrates could be transported linearly through the plasma source by using a roller.

The voltage applied to the multi-pin power electrode was 3 ∼ 10 kV (20 ∼ 30 kHz), and 5 slm of He was used as the discharge gas. The discharge voltage and current were measured using a high-voltage probe (Tektronix P-6015A) and a current meter (Pearson Electronics, 6600), respectively. With an optical emission spectrometer (OES, SC Tech, PCM 420), the optical emission peaks from species such as He (feed gas) and oxygen atoms (from the residual air) were investigated. Also, with photoresist-covered glass substrates, the etching characteristics of the photoresist by the residual oxygen in He were investigated.

III. RESULTS AND DISCUSSION

Fig. 2 shows the discharge current measured as a function of the applied voltage for various pin densities of the power electrode at 5 slm of He. As the figure shows, an increase in the applied AC voltage increased the discharge current. In a corona discharge having a pin-to-plate discharge type, the relationship between the current and the voltage is represented as [15–18]

$$I = 2\pi K\varepsilon/a[F(\delta/a)]^{-2}(V - V_0)^2 \quad (1)$$

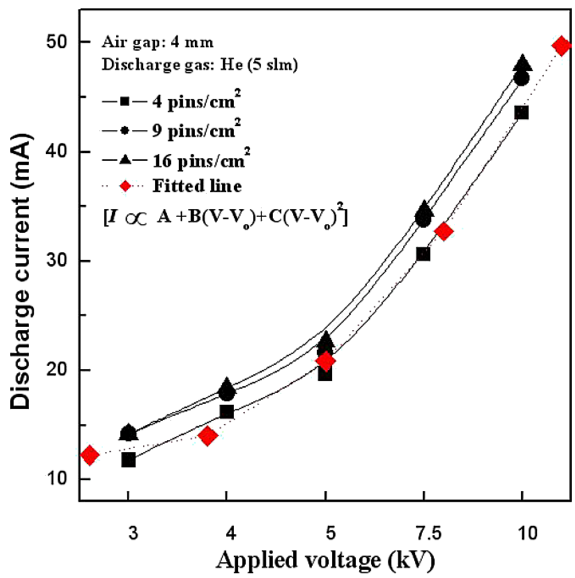

Fig. 2. Discharge current measured as a function of applied voltage for various pin densities of the power electrode at 5 slm of He. The air gap between the electrodes was 4 mm.

where I is the discharge current, K is the charge carrier mobility, ε is the permittivity of the medium, V is the applied AC voltage, and V_0 is the onset voltage. $F(\delta/a)$ represents a series expansion of a function in terms of the ratio of the minimum radius of curvature δ of the corona glow to the pin-to-plane distance a. As in Eq.(1), in the corona discharge, the discharge current I is proportional to the square of the differences between the applied voltage and the onset voltage; that is, $I \propto (V - V_0)^2$. In fact, when the discharge current was calculated from the applied voltage and the onset voltage, the experimental data could be fitted to the above equation. Therefore, the pin-to-plate DBD showed electrical characteristics similar to those of a corona discharge. When the pin density of the multi-pin powered electrode was increased from 4 to 16/cm^2, as shown in the figure, the discharge current was also increased at a given applied AC voltage. For example, when the applied voltage was 10 kV, the discharge currents for pin densities of 4/cm^2, 9/cm^2, and 16/cm^2 were 42 mA, 46 mA, and 49 mA, respectively. Therefore, a fourfold increase in pin density increased the discharge current by about 25 %. In fact, the current flowing in an electric circuit can be determined from the following equation:

$$I = \int J \cdot dA = \int \rho K E \cdot dA \quad (2)$$

Where J is the current density, dA is the elemental surface area, ρ is the charge density, K is the charge carrier mobility, and E is the electric field. Therefore, the current flowing in the circuit should be proportional to the area of the powered electrode. However, in our experimental pin-to-plate plasma source, possibly due to the dielectrics located on both of the electrodes, charging

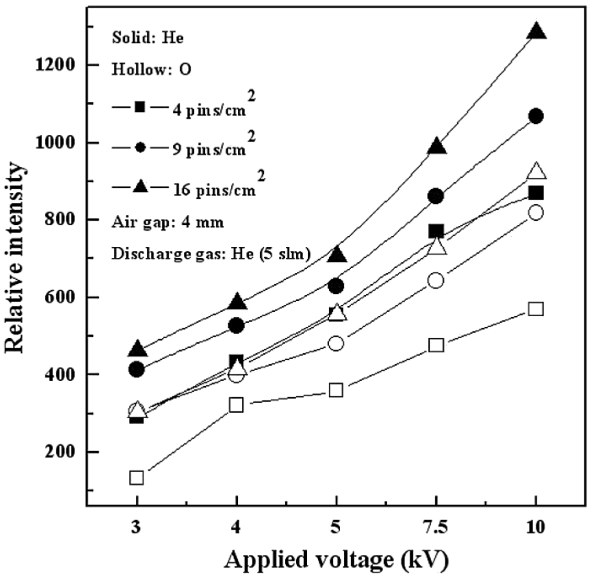

Fig. 3. Optical emission intensities from He metastable and oxygen atoms observed by OES as a function of the applied voltage for different pin densities of the power electrode. The air gap between the electrodes was 4 mm. The oxygen atomic emission intensities originated from the residual air during the atmospheric pressure operation.

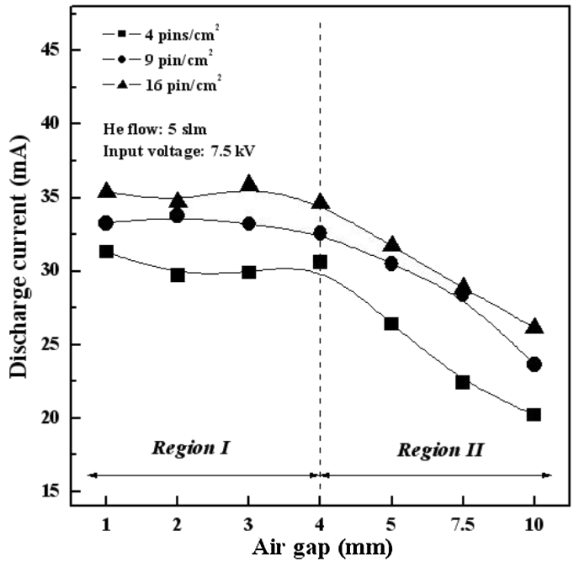

Fig. 4. Discharge current measured as a function of the air gap between the electrodes for various pin densities at an applied voltage of 7.5 kV and a He flow rate of 5 slm.

of the dielectrics can occur, so the discharge area of each pin is partially shielded by the charging; therefore, the electrode area may not be proportional to the current flowing to the electrode. Therefore, the discharge current not being proportional to the pin density appears related to charging on the dielectrics. However, with increasing pin density, there was a definite increase in the discharge current at a given voltage, as shown in the figure.

Using OES, the optical emission intensities from He metastables were observed as functions of the applied voltage for different pin densities of the power electrode, and the results are shown in Fig. 3. The wavelength of the observed He metastable emission peak was 706.5 nm, which originates from the following reactions [19–21]:

$$HE_2^+ + e \rightarrow He_2^* \rightarrow He^*(3n) + He \quad (3)$$

As the figure shows, an increase in the applied voltage increased the optical emission intensities from He metastables, and an increase in the pin density of the powered electrode increased the emission intensity. During the operation of a He atmospheric-pressure plasma, due to the open environment, a small amount portion of air leaked into the system; therefore, the optical emissions from residual oxygen and nitrogen are observed. In the figure, emissions from oxygen atoms are also seen and, an increase in the applied voltage or the pin density increased the optical emission peak intensity from the oxygen atoms, possibly indicating increased dissociation of residual oxygen molecules. An increase in the pin density from 4 to 16 pins/cm^2 increased the He metastable intensity and the oxygen optical emission intensity about 55 %. An increase in the applied voltage increases the power consumed by the source and increases not only the plasma density but also the densities of metastables and dissociated species. An increase in the pin density of the powered electrode also increased the power consumed at a given applied voltage by increasing the discharge current, as shown in Fig. 2. When the consumed power was investigated at an applied voltage of 10 kV, the consumed power at 4 pins/cm^2 was 340 W and that at 16 pins/cm^2 was 460 W. Therefore, the increased dissociations of oxygen molecules and He metastables at higher pin densities are from the increased power consumption at a given applied voltage. A higher consumed power at a given voltage is preferred in flat panel display processing because an increase in the power consumed at a given voltage decreases the chance of transition from a glow discharge to a filamentary discharge and decreases the possibility of damage to the substrate.

Fig. 4 shows the discharge current measured as a function of the air gap between the electrodes for various pin densities of the powered electrode at an applied voltage of 7.5 kV for and 5 slm of He. As the figure shows, an increase in the air gap changed the discharge current insignificantly in the gap-distance range from 1 to 4 mm, but further increases in the gap distance decreased the discharge current. For the pin density, a higher pin density always showed a higher current density. The decrease in the discharge current for air gaps larger than 5 mm was due to the discharge changing from a glow discharge to a filamentary discharge. In region I in Fig. 4 (air gap from 1 to 4 mm), the discharges were stable glow discharges but, in region II (air gap from 5 to 10 mm), the discharges were unstable filamentary discharges. An

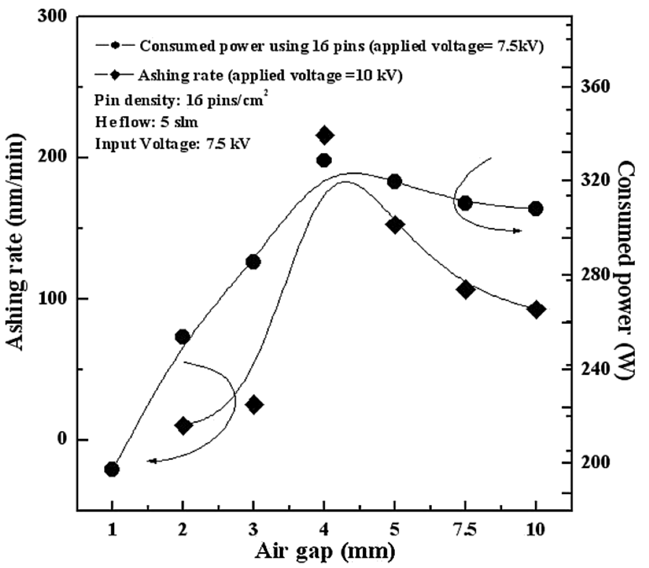

Fig. 5. Calculated consumed power measured as a function of the air gap for 16 pins/cm^2 at an applied voltage of 7.5 kV and a He flow rate of 5 slm. The photoresist ashing rate due to the residual oxygen gas in the He at an applied voltage of 10 kV is also shown.

increase in the discharge gap at a given voltage decreases the electric field in the air gap. In the case of region I, the electric field is believed to be sufficiently strong to generate He metastables. however, in region II, the electric field is no longer sufficiently strong to generate the metastables required for maintaining a glow discharge. The decrease in the number of metastables between the electrodes with increasing air gap increases the chance for a filamentary discharge occurring, possibly by increasing the plasma resistance between the electrodes.

Fig. 5 shows the calculated consumed power measured as a function of the air gap for 16 pins/cm^2 at a 7.5 kV applied voltage for 5 slm of He. The photoresist ashing rate at a 10 kV applied voltage due to the residual oxygen gas in He is also shown. As the figure shows, an increase in the discharge gap from 1 to 4 mm increased the consumed power almost linearly; however, a further increase in the discharge gap decreased the discharge current slightly. The increase in the consumed power increasing air gap up to 4 mm at a given voltage appears to be from the increased plasma volume between the gap while maintaining the discharge current at a given voltage. However, the decrease in the consumed power with a further increase of the air gap is related to a transition to a filamentary discharge and, therefore, to the power only in a small portion of the discharge volume between the electrodes being consumed. The photoresist ashing rate was related to the consumption of power in the discharge volume. As Fig. 5 shows, the photoresist ashing rate increased with increasing gap distance and showed a maximum of 145 nm/min at a 4 mm air gap. A further increase in the gap distance decreased the photoresist ashing rate. Therefore, the variation in the ashing rate with the air gap was similar to that of the power consumption..

IV. CONCLUSIONS

In this study, as an application to next generation flat panel display processing, the characteristics of the pin-to-plate DBD have been investigated as functions of the applied AC voltage, the air gap between the electrodes, and the pin density of the powered electrode. An increase in the applied voltage up to 10 kV increased the discharge current as $I \propto (V - V_0)^2$, similar to the current-voltage characteristics of a pin-to-plate corona discharge and the optical emission intensities from He metastables and residual oxygen atoms, indicating that increased densities of ions, metastables, and dissociated species are caused by the increased power consumption in the plasma. The optimum air gap at a given applied voltage was 4 mm, for which the power consumption was the highest, and further increases in the air gap decreased the power consumption due to the transition from a glow discharge to a filamentary discharge. When the pin density was varied from 4 to 16 pins/cm^2, higher optical emission intensities from He metastables and oxygen atoms were obtained by increasing power consumption at a given applied voltage. The photoresist ashing rate at a given voltage was the highest when the pin density was 16 pins/cm^2 and when the air gap was 4 mm, possibly caused by the dissociated oxygen atomic density in the plasma and the power consumption being highest. A higher power consumption at a given AC voltage is desirable for flat panel display applications because it decreases the chance of transition from a glow discharge to a filamentary discharge and decreases the possibility of damage to the substrate

ACKNOWLEDGMENTS

This work was supported by the National Research Laboratory Program of Korea's Ministry of Science and Technology (MOST).

REFERENCES

[1] H. E. Wagner, R. Brandenburg, K. V. Kozlov, A. Sonnenfeld, P. Michel and J. F. Behnke, Vacuum **71**, 417 (2003).
[2] M. Sugawara, Surf. Coat. Technol. **142**, 290 (2001).
[3] R. Vertriest, R. Morent, J. Dewulf, C. Leys and H. Van Langenhove, Plasma Sources Sci. Technol. **12**, 412 (2003).
[4] I. Suarasan, L. Ghizdavu, I. Ghizdavu, S. Budu and L. Dascalescu, J. Electrostat. **54**, 207 (2002).

[5] Y. H. Lee, C. H. Yi, M. J. Chung and G. Y. Yeom, Surf. Coat. Technol. **146**, 474 (2001).
[6] O. Goosens, E. Dekempeneer, D. Vangeneugden, R. V. Leest and C. Leys, Surf. Coat. Technol. **142**, 474 (2001).
[7] K. Chaudhary, K. Inomata, M. Yoshimoto and H. Koinuma, Mater. Lett. **57**, 3406 (2003).
[8] C. H. Yi, C. H. Jeong, Y. H. Lee, Y. W. Ko and G. Y. Yeom, Surf. Coat. Technol. **177**, 711 (2004).
[9] Y. B. Guo and F. C. N. Hong, Appl. Phys. Lett. **82**, 337 (2003).
[10] S. Y. Moon, W. Choe and B. K. Kang, Appl. Phys. Lett. **84**, 188 (2004).
[11] H. S. Uhm, J. Korean Phys. Soc. **42**, 775 (2003).
[12] J. D. Moon, S. T. Geum, G. T. Lee and D. K. Park, J. Korean Phys. Soc. **38**, 680 (2001).
[13] H. Mase, T. Fujiwara and N. Sato, Appl. Phys. Lett. **83**, 5392 (2003).
[14] K. Yamakawa, M. Hori, T. Goto, S. Den, T. Katagiri and H. Kano, Appl. Phys. Lett. **85**, 549 (2004).
[15] B. Henson, J. Appl. Phys. **53**, 3305 (1982).
[16] B. Henson, J. Appl. Phys. **52**, 3921 (1981).
[17] R. S. Sigmond, J. Appl. Phys. **53**, 891 (1982).
[18] Y. B. Golubovskii, V. A. Maiorov, J. Behnke and J. F. Behnke, J. Phys. D: Appl. Phys. **35**, 751 (2002).
[19] Y. B. Golubovskii, V. A. Maiorov, J. Behnke and J. F. Behnke, J. Phys. D: Appl. Phys. **36**, 39 (2003).
[20] N. K. Bibinov, A. A. Fateev and K. Wiesemann, J. Phys. D: Appl. Phys. **34**, 1819 (2001).
[21] B. M. Kim, J. Korean Phys. Soc. **44**, 427 (2004).